Myosin-II inhibition and soft 2D matrix maximize multinucleation and cellular projections typical of platelet-producing megakaryocytes

Jae-Won Shin[a,b], Joe Swift[b], Kyle R. Spinler[b], and Dennis E. Discher[a,b,1]

[a]Pharmacology Graduate Group, School of Medicine, and [b]Chemical and Biomolecular Engineering, University of Pennsylvania, Philadelphia, PA 19104

Edited by Thomas P. Stossel, Harvard Medical School, Boston, MA, and approved May 27, 2011 (received for review November 23, 2010)

Cell division, membrane rigidity, and strong adhesion to a rigid matrix are all promoted by myosin-II, and so multinucleated cells with distended membranes—typical of megakaryocytes (MKs)—seem predictable for low myosin activity in cells on soft matrices. Paradoxically, myosin mutations lead to defects in MKs and platelets. Here, reversible inhibition of myosin-II is sustained over several cell cycles to produce 3- to 10-fold increases in polyploid MK and a number of other cell types. Even brief inhibition generates highly distensible, proplatelet-like projections that fragment readily under shear, as seen in platelet generation from MKs in vivo. The effects are maximized with collagenous matrices that are soft and 2D, like the perivascular niches in marrow rather than 3D or rigid, like bone. Although multinucleation of other primary hematopoietic lineages helps to generalize a failure-to-fission mechanism, lineage-specific signaling with increased polyploidy proves possible and novel with phospho-regulation of myosin-II heavy chain. Label-free mass spectrometry quantitation of the MK proteome uses a unique proportional peak fingerprint (ProPF) analysis to also show upregulation of the cytoskeletal and adhesion machinery critical to platelet function. Myosin-inhibited MKs generate more platelets in vitro and also in vivo from the marrows of xenografted mice, while agonist stimulation activates platelet spreading and integrin αIIbβ3. Myosin-II thus seems a central, matrix-regulated node for MK-poiesis and platelet generation.

matrix elasticity | blebbistatin | proteomics | thrombocytopenia

Actomyosin forces drive a number of general cellular processes. Fission at the end of cytokinesis is one such process promoted by myosin-II with inhibition of nonmuscle myosin-II (NMM-II) in proliferating cells producing more binucleate and polyploid cells (1). Second, actomyosin forces help to establish an active cortical tension, which stiffens and stabilizes the plasma membrane (2). Inhibition of NMM-II thus tends to cause at least some adherent cell types to exhibit more filipodia-like membrane extensions and appear more dendritic (1). Finally, NMM-II contributes to adhesion as cells attach to ligand and then pull and sense elasticity of their microenvironment, impacting differentiation of both adult (2) and embryonic stem cells (3). These basic functions of myosin are also partially coupled. Membrane or cortical rigidity increases with matrix rigidity as cells apply more tension to adhesion complexes on stiff substrates, promoting focal adhesion growth (2). Cytokinesis is also modulated by cell adhesion (4) with nonspecific attachment overriding the polyploidization described originally for suspensions of myosin-II–null *Dictyostelium* amoeba (5). However, cells in tissues do not grow in suspension: contact and adhesion are unavoidable in vivo. In all of these contexts, megakaryocytes (MKs) are intriguing in that they are polyploid, they exhibit proplatelet extensions suggestive of a highly flexible membrane, and they adhere within a complex bone marrow microenvironment (Fig. 1*A*). MKs also express abundant NMM IIA (*MYH9*) as do MK-generated platelets (6).

Differentiation to MKs in vivo starts with multipotent hematopoietic stem cells (HSCs) that are located at osteoblastic niches on rigid, high collagen bone (7). As MKs mature, they replicate their DNA but do not divide, a process termed endomitosis, and they also migrate into the soft marrow space and into perivascular niches (8). MKs do not transmigrate into blood, perhaps because their polyploid nuclei are too large and rigid, but they do extend tubular membrane projections, known as proplatelets, into blood, where shear flow fragments the extensions to generate circulating platelets (8). In case of injury to a vessel wall or perhaps other activating signals, platelets adhere to the wall or to a multiplatelet thrombus and use actomyosin forces to contract the thrombus and form a tight seal on the wall. We hypothesized that sustained inhibition of NMM-IIA together with soft matrices would maximize both MK maturation and proplatelet generation, and we sought insight into possible pathways of molecular regulation. Quality platelets for transfusion—as needed for various interventions (radiation, surgery) and diseases (leukemia)—are also supply-limited (9).

Human mutations in *MYH9* cause May-Hegglin anomaly, with large platelets that are reduced in number as thrombocytopenia (10, 11). In mouse, deletion of *MYH9* in MKs also produces May-Hegglin–like defects (12, 13). Paradoxically, pharmacological inhibition of NMM-II ATPase by blebbistatin in mouse adult (13) and mouse embryonic (14) systems is reported to produce a two- to ~threefold increase in proplatelet extensions but not affect MK ploidy or size, at least for the doses or times tested. Whether human MK-poiesis is regulated by myosin-II has remained unclear, but possible pathways include direct phosphorylation of NMM-II (i.e., heavy-chain regulation that decreases myosin activity in other cells) (15). Rho-associated protein kinase can affect myosin-II and is known to increase MK ploidy by approximately twofold (14). Here, NMM-IIA's role in MK maturation and subsequent platelet production is examined directly starting with human bone marrow (BM)-derived $CD34^+$ cells cultured with just two cytokines to differentiate into MK progenitors followed by sustained reversible inhibition of myosin-II for 3 d (Fig. 1*B*).

Results and Analysis

Myosin-II Inhibition Increases MK Polyploidy and Membrane Fragmentability. Mature polyploid MKs are increased in number by 3- to ~10-fold by blebbistatin, without affecting total MKs. Polyploid MKs are $CD41^+$ (CD41: $\alpha_{2b}\beta_3$-integrin) with a high multiple of chromatin pairs per cell (≥8 N) (Fig. 1*C*). Sustained application of drug also depletes the pool of MK progenitors, with responses that are all highly cooperative in drug concentration (Hill exponents: $n \sim 7$) with similar inhibition constants K_i (~7.6 μM). K_i is approximately twofold higher than blebbistatin inhibition of purified NMM-IIA (1), but the relatively small difference in K_is likely reflects the shift toward higher cooperativity in cell division. Importantly, polyploidization upon sustained inhibition of NMM-II seems to generalize to both human-derived hematopoietic THP-1

Author contributions: J.-W.S. and D.E.D. designed research; J.-W.S., J.S., and K.R.S. performed research; J.-W.S., J.S., and D.E.D. analyzed data; J.S. and K.R.S. contributed new reagents/analytic tools; and J.-W.S., J.S., and D.E.D. wrote the paper.

The authors declare no conflict of interest.

This article is a PNAS Direct Submission.

[1]To whom correspondence should be addressed. E-mail: discher@seas.upenn.edu.

This article contains supporting information online at www.pnas.org/lookup/suppl/doi:10.1073/pnas.1017474108/-/DCSupplemental.

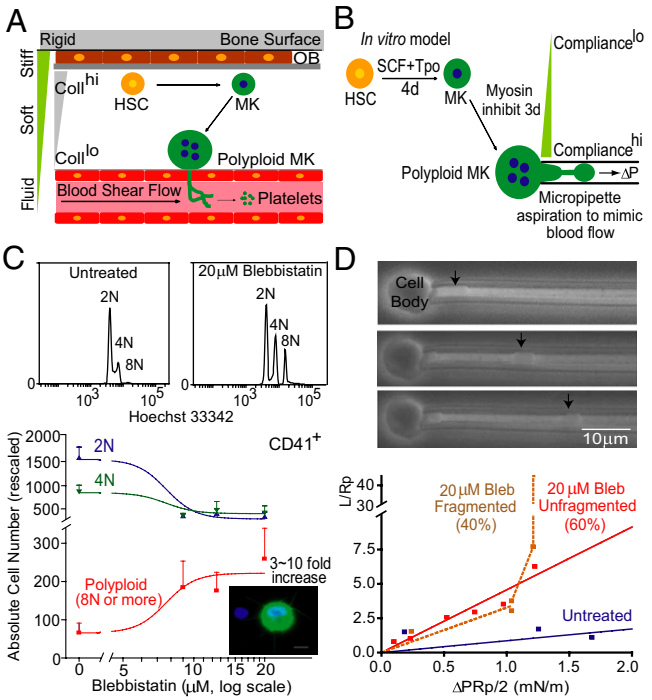

Fig. 1. Myosin affects MK maturation and cell fragmentation. (*A*) In vivo scheme of MK-poiesis and platelet fragmentation in bone marrow. (*B*) Modeling MK maturation and platelet fragmentation in vitro by myosin inhibition and micropipette aspiration on $CD34^+$-derived cultures. (*C*) Myosin inhibition by blebbistatin accelerates $CD41^+$ MK polyploidization. Representative flow cytometry plots for ploidy analysis (*Upper*), and dose-dependence (*Lower*). Absolute values were normalized to 10^4 initial cell input ($n \geq 4$ donors, ± SEM). (*D*) Myosin inhibition increases membrane extension and fragmentation in micropipette aspiration. Representative fragmentation within seconds (*Upper*) after 30 min of 20 μM blebbistatin treatment and aspiration ΔP = 1.4 kPa. Aspiration length vs. effective cortical tension (*Lower*) with median results shown (Fig. S2*A*).

cells and monkey-derived epithelial COS-1 cells (Fig. S1 *A* and *B*). THP-1 cells express NMM-IIA primarily (15), and lentiviral-knockdown using shRNA also increases polyploidy (Fig. S1*C*). COS-1 cells express NMM-IIB almost exclusively, and knockdown by siRNA transfection likewise increases polyploidy (Fig. S1*D*). Polyploidy is therefore not a pharmacological artifact of blebbistatin.

To investigate the additional role of myosin in membrane integrity under shear, cells were subjected to micropipette aspiration with stepwise decreases in pressure using pipettes similar in diameter to human capillaries (~3 μm). The cell and its membrane shear and flow into the micropipette, resembling, in shape, elongated proplatelets. After just 30 min of blebbistatin, cells are approximately fourfold more compliant (Fig. 1*D* and Fig. S2*A*), and 40% of treated cells also rapidly fragment to average sizes similar to those of large human platelets (3 to ~4 μm). Platelets are now known to be generated by shearing of proplatelets (16), and no fragmentation was observed in untreated cells. Projection lengths up to the point of divergent fragmentation vary from 10 to ~20 μm, which is similar to in vivo fragmented proplatelet lengths of ~14 μm (8). Fragmentation stresses here correspond to effective membrane tensions of ~1 mN/m, which is 10-fold lower than cell membrane lysis tensions (17). Platelets not only maintain membrane integrity but also exhibit characteristic structures, such as cortical, coil-like microtubules (MTs), and so we also aspirated primary MKs and MEG01 cells (an MK-like line) after labeling with a very low and cell-viable dose of fluorescent-Taxol (10 nM) (18). Even at a 1,000-fold higher dose of Taxol, proplatelets are known to extend (19). In slow aspirations here, MT-coils could be visualized extending into the projection tips at ~0.7 μm/min (Fig. S2) and bundles of MTs appear more likely than individual MTs, all consistent previously reported rates and structures (19). Although final structures are rate- and force-dependent as transition rates ~ exp(force) (17), the basic findings here indicate both nonlytic fragmentation under shear and MK polyploidization could be promoted in part by myosin inhibition, even with microtubule polymerization as reported (19).

Soft Matrix with Low Collagen Maximizes MK Polyploidy. Cell interactions with extracellular matrix (ECM) are unavoidable in vivo, and such interactions are modulatory, as found originally with substrate-assisted cytokinesis of myosin-null *Dictyostelium* (5). Furthermore, it seems inevitable in BM (Fig. 1*A*) that migrating MKs encounter gradients in both tissue elasticity and collagen density (20). The bone surface is high in collagen-I ($collagen^{hi}$) and stiff, with an estimated elasticity E_{ECM} for osteoid of ~34 kPa (2), whereas the marrow space is $collagen^{lo}$ and very soft, approximated here with E_{ECM} = 0.3 kPa (21). MKs express two collagen receptors: GPVI and integrin-α2β1 (22, 23). Previous results indicate that collagen suppresses maturation of MKs in vitro (24), and so we hypothesized that a low collagen, compliant ECM favors MK polyploidization. $CD34^+$ cells were cultured on polyacrylamide gels of controlled stiffness with different collagen concentrations per previous studies with BM-derived mesenchymal stem cells (2), which showed matrices as soft as muscle are myogenic, whereas matrices that are stiff like osteoid induce osteogenesis.

At low collagen (2 ng/cm^2) and on soft gels (0.3 kPa), polyploid MK increase (by 50%) compared with stiff gels (34 kPa), indicating roles of matrix elasticity in regulating polyploidy (Fig. 2*A*). This effect is maintained over a range of collagen concentrations (2–200 ng/cm^2) (Fig. 2*B*), but is abolished by blebbistatin except for the lowest collagen (2 ng/cm^2). Above a matrix ligand threshold, cells can sense elasticity via myosin (plus other mechanisms, per Fig. 2*A*). These processes are fully decoupled in suspension cultures (Fig. 1*C*).

Because adhesion opposes polyploidy of myosin-null amoeba (4), we further tested—by a simple inversion of submerged cultures (1 g for 30 min)—whether increased adhesion could explain reduction in polyploid MK numbers on stiff gels. Although standard plastic-dish cultures under serum-free conditions show no attachment and are thus suspension cultures, 50% more cells remained anchored to stiff matrices versus soft matrices, with the greater adhesion depending on active NMM-II (Fig. 2*C*). Nonetheless, adhesion to all collagenous gels with or without myosin inhibition was at least 20-fold higher than the near-zero attachment to plastic. Understandably, polyploidy increases (almost twofold) with increasing collagen concentration on stiff gels as cells anchor so strongly that they cannot migrate away to complete division (Fig. 2*D*). Migration is well-known to be biphasic in adhesive ligand, with low ligand promoting migration but high ligand leading to immobilization. Matrix ligand density and stiffness therefore factor in as cells complete cytokinesis by crawling apart, even when myosin is ablated (5).

Soft 2D Collagenous Matrices Are Better than Stiff or 3D. For some cells but not all, NMM-II inhibition causes a dendritic morphology on rigid substrates (1), and this is true of the COS-1 cell line too (Fig. S3 *A–D*), which also stains positive with a dye for lipid "demarcation" membranes within polyploid MKs, even though some major differences are expected between lineages (Fig. S3*E*) (25). The morphology effects are reminiscent of blebbistatin, causing an increased number of MKs with proplatelet extensions when cells are grown on plastic (13, 14), and we indeed find an approximately threefold increase in mean length of proplatelet extensions under such conditions (Fig. 2*E*). Live imaging shows the average proplatelet extension velocity is ~1 μm/min, consistent with a previous study (16) (Fig. S3 *F* and *G* and Movie S1*A*).

Soft collagenous gels—in both 2D and 3D—facilitate proplatelet extensions compared with stiff gels (Fig. 2*E*). Blebbistatin has a considerable additive effect only with 2D soft matrices, with the drug having no effect on cells in 3D collagen gels or on stiff,

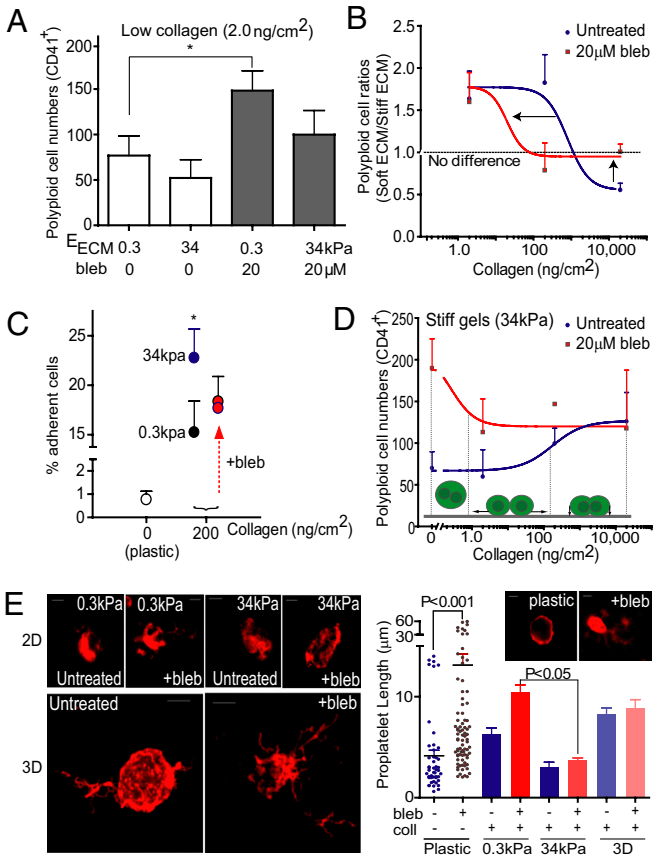

Fig. 2. Effects of matrix elasticity and ligand density on MK polyploidy. All MK polyploid cell numbers were scaled to 10^4 initial cell input ($n \geq 3$ donors; ± SEM). (*A*) Soft (0.3 kPa) matrices always facilitate MK polyploidization on 2 ng/cm^2 (low) collagen gels. Tukey's HSD Test indicates $P < 0.05$ for all pairs except 0.3 kpa 0 μM vs. 34 kpa 20 μM. (*B*) On a range of collagen concentrations, ratios of polyploid MK numbers for soft (0.3 kPa) versus stiff (34 kPa) matrices fit to standard dose-response curves: untreated and blebbistatin-treated IC50 ~20, 1,000 ng/cm^2, respectively (Hill coefficients ~ −1.5, −2.0 respectively). (*C*) Cell adhesion on soft and stiff matrices after 3 d cell culture ± blebbistatin. *$P < 0.05$ for 0.3 kPa vs. 34 kPa untreated. (*D*) Polyploid MK numbers on stiff gels cultured on a range of collagen concentrations. Dose-response curves are shown for untreated (EC_{50} ~200 ng/cm^2, Hill coefficient = 1.0) and blebbistatin-treated cells (IC50 ~0.3 ng/cm^2, Hill coefficient = −1.3). Cartoon depicts effects on cell adhesion and division. (*E*) Proplatelet formation with different gels. (*Left*) Representative images with F-actin (red). (Scale bar, 5 μm.) (*Right*) Quantitation of branch length from cell body. (>50 measurements for each group, $n \geq 2$ donors). 3D matrices are soft with E ~1 to 3 kPa. *P* values are reported from Tukey's HSD test.

osteoid-like matrices. Perhaps the major difference between 2D soft and pure 3D matrix is the high density of ligand in 3D, and as with polyploidy, high collagen tends to anchor and suppress any effect of blebbistatin (Fig. 2*D*).

Myosin-II Heavy Chain Is the Best Target for MK Maturation. For drug treatment times much shorter than the doubling time (~18 h), cells continue to divide and a low number of polyploid MKs are generated. For longer treatment times, however, division is indeed inhibited and more polyploid MKs are generated (Fig. 3*A*). Polyploid cell numbers grow exponentially with duration of drug exposure, and the doubling time for polyploidization proves consistent with drug-free cell proliferation. Other contractility inhibitors are much less effective (Fig. S4*A*). In addition, stem-cell factor (SCF) and thrombopoietin (Tpo) favor MKs, but addition of G-CSF plus blebbistatin produces polyploid CD41$^-$ cells (Fig. S4 *B* and *C*), and time-lapse imaging shows most cells reverse cytokinesis (Fig. 3*B* and Movie S1*B*). Restriction of endomitosis to MKs thus suggests lineage-specific signaling to myosin.

Phospho-Regulation of NMM-IIA and Polyploidy. NMM-II is of course abundant in platelets as well as MKs (6), but phospho-regulation of myosin heavy chain remains a topic of active study. Phosphorylation of S1943 is downstream of EGF receptor, inactivates myosin in epithelial cells, and impacts cell motility (26). PDGF is one known ligand of EGF receptor (27) and reportedly increases the number of MK progenitors (28). Mass spectrometry (MS) analyses of primary cells revealed approximately eightfold more phospho-S1943 in MKs vs. non-MK (CD41$^-$) cells (Fig. 4*A* and Dataset S1*A*), suggesting myosin inactivation accompanies MK differentiation. THP-1 cells immunoprecipitated with an antibody against NMM-IIA (Fig. S5) show blebbistatin increases phospho-S1943 when NMM-IIA is a detergent-soluble monomer rather than polymer (Fig. S6*A* and Dataset S1*B*). This finding is consistent with pSer-deactivation of myosin through inhibition of polymerization (26).

Phosphorylation of Y277 has been implicated in B-cell function (29), and phosphorylation of both Y277 and Y1805 activates myosin for phagocytosis by macrophages (15). Because inhibition or knockdown of NMM-IIA in THP-1 cells caused a major increase in polyploidy (Fig. S1*A*), we examined pTyr in THP-1 and find that blebbistatin decreases pTyr levels under both basal and phosphatase-inhibited conditions. The difference is apparent in NMM-IIA's head plus proximal tail (a 150-kDa fragment) as characterized by immunoprecipitation (IP) (Fig. 4*B*) followed by detailed MS analysis (Fig. S5). Most tryptic peptides from the IP were from NMM-IIA (Dataset S1*C*). Myosin inhibition thus feeds back into signaling pathways.

Given the opposite roles of tyrosine (activating) and serine (deactivating) phosphorylation in modulating myosin activity, we studied which phospho-sites in NMM-IIA might regulate ploidy by taking advantage of the easily transfectable COS cell lines that were previously used to study roles of NMM-II isoforms in cytokinesis (see *SI Materials and Methods*). Because inhibition or knockdown of NMM-IIB in COS-1 cells increases polyploidy (Fig. S1*B*), NMM-IIA heavy chain phospho-mutants were expressed in native COS-1 and in the knockdowns (Fig. 4*C*). The head mutant Y277F increases the number of polyploid cells by approximately twofold (Fig. S6*B*), but phospho-mimetic mutant Y277D abolishes this effect. The pTyr mutant Y1805F in the tail also has no effect

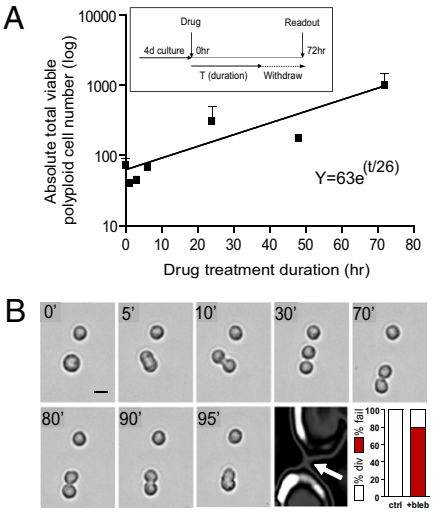

Fig. 3. Sustained inhibition of myosin-II blocks cytokinesis. (*A*) Generation of polyploid cells is exponential in duration of exposure to 20 μM blebbistatin with doubling time of 18.2 h. All values were scaled to an initial cell input of 10^4 cells ($n = 3$, ± SEM). (*B*) Live cell imaging shows reversal of cytokinesis with blebbistatin for ~80% of cells observed; without drug, all cells divided. (Scale bar, 10 μm.)

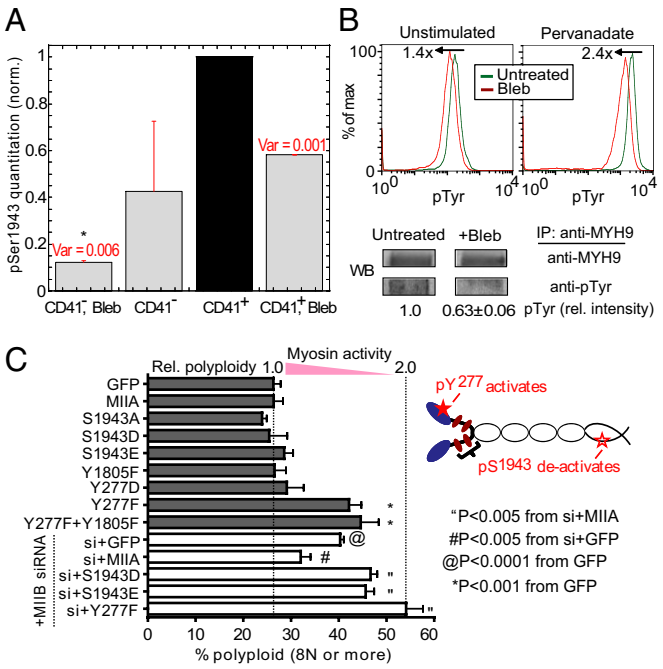

Fig. 4. Phosphorylation of NMM-IIA regulates polyploidization. (*A*) MS analyses of phospho-S1943 in primary cells. Each pS1943 signal was normalized first to total NMM-IIA signal, which was then normalized to values from CD41$^+$ sorted cells (untreated), and averaged between experiments (n = 2). Ion current of pS1943 in CD41$^+$ is ~1% of total NMM-IIA signal. *$P < 0.05$ from one-way ANOVA with Tukey's HSD test. (*B*) Blebbisatin treatment leads to overall reduction of pTyr levels under both unstimulated and pervanadate (100 μM)-stimulated conditions as assessed by flow cytometry (*Upper*). IP of NMM-IIA from lysates of cells treated with pervanadate ± blebbistatin, followed by immunoblot of pTyr and densitometry (*Lower*) shows reduced pTyr levels in NMM-IIA head (150 kDa) region (n = 3, ± SEM). (*C*) NMM-IIA head pTyr mutant (Y277F) increases polyploidization. COS cells were transfected as indicated ± pretransfection with NMM-IIB siRNA. Cultured cells were stained with Hoechst 33342 to quantify polyploidy (≥8 N) by flow cytometry ($n \geq 3$, ± SEM).

on ploidy, but the double mutant Y277F-Y1805F has the same effect on polyploidy as the head mutant. Knockdown of NMM-IIB with siRNA (Fig. S1*D*) shows the expected trends: polyploidy of GFP-transfection controls exceeds native levels, whereas wild-type NMM-IIA rescues partially with suppression of polyploidy. The Y277F mutant acts as a dominant negative (on residual NMM-IIB) and produces the highest levels of polyploidy, with 50% of cells showing ≥8 N. Overexpression of phospho-mimetic serine mutants of NMM-IIA, S1943D and -E, also prevents significant rescue of polyploidy, suggesting pS1943 functionally regulates myosin activity and ploidy. Visualization of the various GFP-NMM-IIA constructs shows the wild-type to be structured in cells, perhaps like stress fibers, but the Y277F mutant is far more diffuse (Fig. S6*C*). The results thus identify at least two specific signaling targets in myosin heavy chain that can regulate polyploidization, thereby implicating upstream signaling pathways in the marrow's perivascular niches for MKs.

Proteomic Profile of Blebbistatin-Treated MKs Is Platelet-Like. Because blebbistatin promotes maturation of CD41$^+$ cells in terms of ploidy and proplatelets, the proteomic profile of drug-treated cells might be expected to better approximate that of platelets, which have been extensively profiled (Dataset S1*D*). Using a unique label-free analysis of proteomes based on proportional peak fingerprints (ProPF) (see *SI Materials and Methods*) and motivated by the reported up-regulation in MKs of 22 actin cytoskeleton genes, five α- and β-tubulin isoforms, and just one down-regulated actin cytoskeletal gene (30), we quantified all cytoskeletal proteins for which three or more tryptic peptides were detected in four distinct cell lysates: CD41$^-$, CD41$^+$, drug-treated, and not drug-treated (Fig. S7 *A* and *B*). CD41$^-$ cells include many hematopoietic cells that are CD34^{hi}, a marker of HSCs and progenitors of various lineages (Fig. S7*C* and Dataset S1*E*). Normalization to untreated CD41$^-$ cells shows blebbistatin has little effect, increasing expression modestly of only 20% of the indicated proteins (Fig. 5). In contrast, CD41$^+$ cells show considerable up-regulation: 50% of detected proteins in untreated samples and 75% in treated samples are up. This finding suggests an increasing level of differentiation especially in contractility with heavy and light myosin-II chains, and also adhesion linkers talin and vinculin (detected proteins in Dataset S1 *E* and *F*). Tubulin α- and β-isoforms are also slightly up and to a similar extent as expected of heterodimers. Validation of the proteomics with antibodies against key proteins, including NMM-IIA and vinculin (Fig. S7*D*), proved consistent with mRNA up-regulation of NMM-IIA and vinculin in MKs (30).

Reversible Inhibition of NMM-II Increases Functional Platelet Numbers. Transplantation of uncultured human cord-blood CD34$^+$ cells in immuno-deficient nonobese diabetic (NOD)/SCID mice has been shown previously to yield sustained generation of human platelets (31), but the intravenous delivery route used to date requires a large number of cells for homing and engraftment. Intrabone marrow transplantation was instead used here to more rapidly expose injected cells to the marrow microenvironment per Fig. 1*A*. Nucleated cellular fractions of CD34$^+$ cells cultured with SCF and Tpo with or without blebbistatin were xenografted into NOD/SCID/IL-2Rγ$^{-/-}$ (NSG) mice, and human MK were indeed detectable within the tibia and not lung or spleen at day 3 post-transplant (Fig. S8*A*). Subsequent quantification of circulating human-CD41$^+$ platelets at day 3 indicates that human cells treated ex vivo with blebbistatin generate more in vivo human platelets per transplanted CD41$^+$ cell by about fourfold (Fig. 6*A*, *Left*). These in vivo-generated platelets derive from CD41$^+$ cells because CD34$^+$ cells do not generate platelets until after 2 wk (31). To determine if the in vivo observations could be recapitulated in vitro, MKs exposed to blebbistatin for 3 d were washed and the nucleated cell fraction was isolated by a density gradient to remove any existing fragments (32), followed by further culture with Tpo

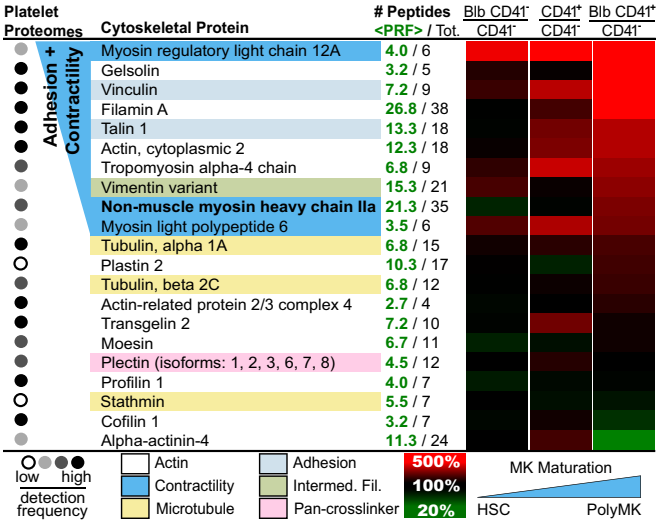

Fig. 5. Label-free MS quantitation of myosin-inhibited cytoskeletal proteome. CD34$^+$ cells were treated with blebbistatin for 3 d. The viable cell fraction (Annexin-V$^-$ and 7-AAD$^-$) of CD41$^+$ MKs was isolated by sorting, followed by MS (see *SI Materials and Methods*, Fig. S7*B*, and Dataset S1*D*). The first column summarizes detectability in prior literature on platelets. <PRF> refers to the number of peptides retained in propotional peak fingerprint for protein quantitation, whereas "Total" refers to all peptides detected.

for 3 d. Counting the in vitro-generated, platelet-sized fragments indicates that blebbistatin-exposed MKs generate 2.5-fold more in vitro platelets per CD41$^+$ cell than untreated MKs (Fig. 6*A*, *Right*).

Human platelet-like fragments derived from both untreated and blebbistatin-exposed MKs show cortical, coil-like MT structures as seen in some human blood-derived platelets (Fig. 6*B*). Furthermore, unlike platelets derived from patients with May-Hegglin anomaly (33), platelets derived from blebbistatin-exposed MKs as well as MKs themselves do not exhibit reduced CD42b expression compared with untreated controls and blood platelets; the CD42b to CD41 mean fluorescent intensity ratio remains similar (Fig. S8*B*). In vitro-generated platelets are not subjected to fluid shear and are expected to be larger, as seen in imaging (Fig. 6*C* and Fig. S8*C*), with higher CD41 and 42b intensities (Fig. S8*B*) and higher forward scatter compared with blood platelets. Reversible but sustained NMM-II inhibition thus does not compromise MK and platelet structure or surface marker expression (Fig. 5 and Fig. S7*D*).

Regardless of blebbistatin treatment, MK-derived platelets are capable of forming filopodia on collagen-I matrix upon thrombin stimulation (at 1 U/mL) (Fig. 6*C*). F-actin also reorganizes through αIIbβ3 integrin outside-in signaling, as revealed by formation of filopodia, lamellipodia, and stress fibers on fibrinogen upon thrombin stimulation (at 1 U/mL) (Fig. S8*C*). MKs themselves spread and form stress fibers on fibrinogen regardless of blebbistatin treatment (Fig. S8*D*), as reported for murine ESC-derived MKs (34). Furthermore, the active conformation and clustering of human αIIbβ3, which binds fibrinogen, was directly confirmed with PAC-1 antibody binding upon stimulation of platelet-like fragments derived from both untreated and blebbistatin-treated MKs (Fig. 6*D*). Specificity of agonist-induced PAC-1 binding was verified by inhibiting αIIbβ3 activation with tirofiban (10 μM) per Takayama et al. (35). Blebbistatin-exposed MK-derived in vitro platelets thus preserve major functional responses of blood-derived platelets. Additionally, human platelets obtained from NSG mouse transplants of MKs (Fig. 6*A*, *Left*) show activation by known agonists (ADP, PMA, and thrombin) of P-selectin expression (Fig. S8*E*). Levels are similar to those reported for human platelets generated in NOD/SCID mice 2 wk after transplantation of CD34$^+$ cells (31). The results thus indicate that transient ex vivo inhibition of NMM-II by the protocol here increases the number of functional human platelets.

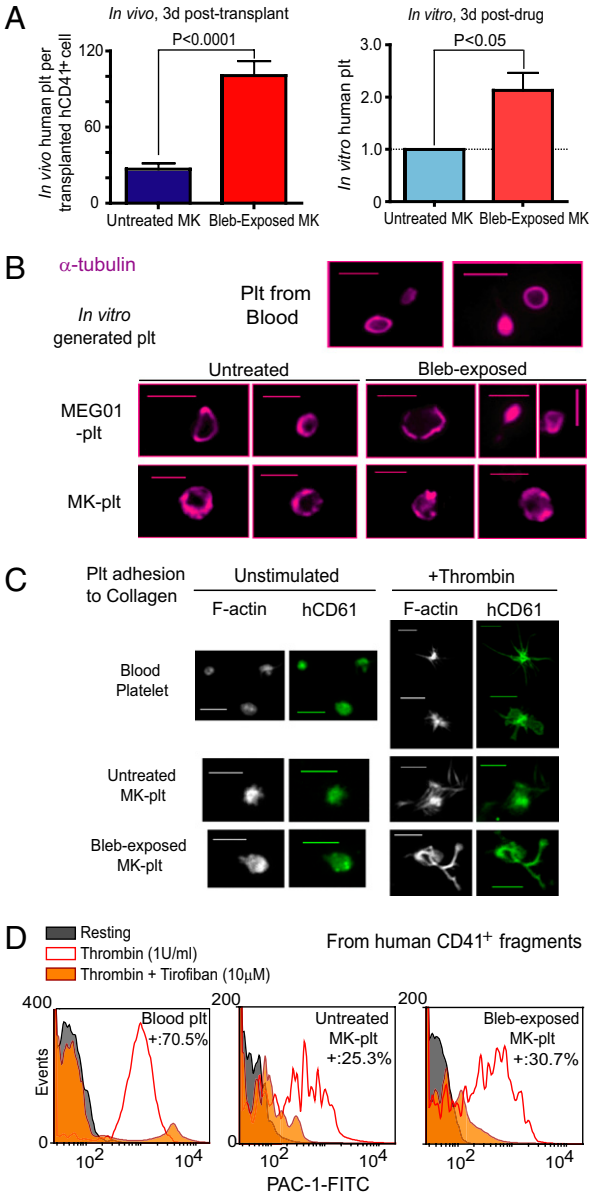

Fig. 6. Platelets derived from myosin-inhibited MKs. (*A*) Platelets per CD41$^+$ cell. (*Left*) NSG mice transplanted intratibially with human-CD34$^+$-derived cells that were pretreated ex vivo with blebbistatin for 3 d (versus untreated cells) show enhanced circulating human platelets. ($P < 0.0001$; $n = 9$ mice ± SEM). (*Right*) MKs exposed to blebbistatin (20 μM for 3 d, then 3 d of no drug) show more in vitro platelets ($P < 0.05$; $n = 5$ donors, ± SEM). (*B*) Similar immunostaining of microtubules in the various MK-derived platelets ($n = 3$ donors). (*C*) Similar adhesion and filipodia formation of various MK-derived platelets on collagen-I upon thrombin (1 U/mL) stimulation. ($n = 3$ donors). (*D*) Platelets derived from blebbistatin-exposed MKs show normal PAC-1 binding with thrombin (1 U/mL). Tirofiban (10 μM) selectively antagonizes αIIbβ3 and inhibits as expected (35). Representative flow cytometry plots from three experiments. (Scale bars, 5 μm.)

Discussion

Deletion of the one myosin-II gene in *Dictyosteum* causes multinucleation of cells in suspension, but division proceeds with cells on glass coverslips via traction-mediated motility (4). This finding is critical to understand more thoroughly because adhesive attachment in tissues, such as BM, is unavoidable (Fig. 1*A*). Here, inhibition of NMM-IIA over several cell cycles invariably enhances polyploidization of primary human-MKs (Fig. 1*C*), as well as G-CSF–induced CD34$^+$ cells (Fig. S4 *B* and *C*), COS-1s, and THP-1s (Fig. S1). The effect on MKs is maximized when grown on marrow-mimetic soft matrices with low collagen density (Fig. 2). Stiff or rigid, ligand-coated matrices are well known to strengthen adhesion by mechanisms that at least involve myosin-II–dependent growth of focal adhesions (2). Soft matrices here nonetheless show adherent cell numbers are still ~2,000% above nonspecific attachment to plastic, but adherent cell numbers on stiff matrices are only about 50% higher (Fig. 2*C*), with blebbistatin suppressing the difference. Anchorage to stiff matrix is thus not only detectably stronger but stiff, collagen^{hi} matrix even promotes polyploidy (~twofold) relative to MK on plastic (Fig. 2*D*), presumably through anchorage-limited motility. Blebbistatin is nonetheless more potent to cells on soft collagen^{lo} matrix, which minimizes adhesion-facilitated motility, and thereby maximizes polyploidy.

Mouse ESC-derived MKs treated with blebbistatin (14) did not show higher polyploidy, probably because treatment duration was too brief relative to cell cycle (Fig. 3*A*). In addition, drug doses of ~100 μM are 20-fold above the K_i (Fig. 1*C*) and in a range that we find to be toxic, indicative of off-target effects (see *SI Materials and Methods*). Lineage-specific NMM-IIA knockout mouse models also did not show increased polyploidy in previous studies (12), probably because the knockout is irreversibly sustained; our 3-d treatment is long relative to cell cycle but not so long that off-target effects accumulate and undermine cell viability. A physiological pathway of myosin-II deactivation (Fig. 4) conceivably involves transient signaling from lineage specific upstream factors, which remain to be identified. Y277 on the myosin-II head involves SHP-1/2 phosphatase (29), and S1943 in the tail is downstream of growth factors (perhaps PDGF). The drug approach here mimics

such niche signaling to maintain cell viability and even enhance myosin protein levels in MKs (Fig. 5).

The activity of NMM-II typically contributes a cortical tension that stiffens and stabilizes the plasma membrane (2), and so inhibition of NMM-II understandably causes at least some adherent cell types to generate more filipodia-like extensions (1), as seen here also with COS-1 cells (Fig. S3 *A–D*). In addition, with strongly adherent cells, NMM-II is activated into stress fibers on rigid matrices (2), and so a soft, collagen^{lo} matrix would seem optimal to minimize adhesive activation of NMM-II. For these reasons, blebbistatin-treated MKs on the marrow-mimetic soft, collagen^{lo} matrix are optimal for proplatelet extensions (Fig. 2*E*). Micropipette aspiration indeed demonstrates that myosin inhibition allows fluid forces to extend and fragment cell membranes (Fig. 1*D*), while aspiration also bends and distends microtubule loops (Fig. S2). This finding is fully consistent with the emerging picture (Fig. 1*A*) that proplatelet extensions into blood flow permit shear fragmentation to generate circulating platelets (8). A similar magnitude of softening with myosin inhibition was also documented with mesenchymal stem cells (2) as well as in natural MK maturation (36).

MK maturation involves changes in the proteome (Fig. 5) that fit a remodeled, platelet-generating phenotype. Adhesion proteins up-regulated in CD41$^+$ cells, with or without blebbistatin, include talin and vinculin, indicative of an adherent phenotype. Blebbistatin-treated CD41$^+$ cells up-regulate NMM-IIA, myosin light chains, and also actin and tropomyosin which seems consistent with previous results showing myosin inhibition reduces actin turnover and leads to F-actin stabilization (37), contributing to membrane extensions. Microtubules also show a tendency to polymerize into such extensions, as seen in proplatelets (Fig. S2*B* and Fig. 3*D*) (16), and CD41$^+$ cells are indeed seen here to up-regulate α- and β-tubulin heterodimers.

MKs exposed to blebbistatin for several days generate platelets with a morphology and activatable-functionality similar to those from untreated MKs and approximating blood platelets. Increased functional platelet number is therefore a result of NMM-II inhibition of MKs. The NMM-II inhibition here is reversible after drug washout (1) and, given the abundance of NMM-II in platelets (6), it seems more likely that the irreversible deficiencies or mutations of NMM-II in May-Hegglin anomaly will undermine platelet function, as observed clinically with macrothrombocytopenia and reduced surface platelet proteins, such as CD42b (33). Results here thus implicate regulated NMM-II coupled to a soft marrow-mimetic matrix in the polyploidization of MKs and in membrane softening with proplatelet extensions, ultimately amplifying platelet numbers in vivo.

Materials and Methods

Details of cell culture, micropipette analysis, construction of collagen-coated gels, and other techniques are in *SI Materials and Methods*. Cells from >10 different donors were used. Our unique label-free MS quantitation of protein (developed by J.S.) uses peptide ion currents from those peptides that maintain proportionality within and between samples.

ACKNOWLEDGMENTS. We thank Dr. Mortimer Poncz and Dr. Paul Janmey for careful reading, Dr. Charles Abrams for platelet discussions, and Drs. Anne Bresnick and Manorama Tewari for providing GFP-MIIA-S1943D/E and GFP-MIIA-Y277D. This study was supported by the American Heart Association (J.-W.S.), National Institutes of Health (P01DK032094 and R01HL062352), and the Human Frontier Science Program (D.E.D.).

1. Straight AF, et al. (2003) Dissecting temporal and spatial control of cytokinesis with a myosin II Inhibitor. *Science* 299:1743–1747.
2. Engler AJ, Sen S, Sweeney HL, Discher DE (2006) Matrix elasticity directs stem cell lineage specification. *Cell* 126:677–689.
3. Conti MA, Even-Ram S, Liu C, Yamada KM, Adelstein RS (2004) Defects in cell adhesion and the visceral endoderm following ablation of nonmuscle myosin heavy chain II-A in mice. *J Biol Chem* 279:41263–41266.
4. Zang JH, et al. (1997) On the role of myosin-II in cytokinesis: Division of *Dictyostelium* cells under adhesive and nonadhesive conditions. *Mol Biol Cell* 8:2617–2629.
5. De Lozanne A, Spudich JA (1987) Disruption of the *Dictyostelium* myosin heavy chain gene by homologous recombination. *Science* 236:1086–1091.
6. Maupin P, Phillips CL, Adelstein RS, Pollard TD (1994) Differential localization of myosin-II isozymes in human cultured cells and blood cells. *J Cell Sci* 107:3077–3090.
7. Calvi LM, et al. (2003) Osteoblastic cells regulate the haematopoietic stem cell niche. *Nature* 425:841–846.
8. Junt T, et al. (2007) Dynamic visualization of thrombopoiesis within bone marrow. *Science* 317:1767–1770.
9. Tinmouth AT, Freedman J (2003) Prophylactic platelet transfusions: Which dose is the best dose? A review of the literature. *Transfus Med Rev* 17:181–193.
10. Kelley MJ, Jawien W, Ortel TL, Korczak JF (2000) Mutation of MYH9, encoding non-muscle myosin heavy chain A, in May-Hegglin anomaly. *Nat Genet* 26:106–108.
11. Seri M, et al.; The May-Heggllin/Fechtner Syndrome Consortium (2000) Mutations in MYH9 result in the May-Hegglin anomaly, and Fechtner and Sebastian syndromes. *Nat Genet* 26:103–105.
12. Eckly A, et al. (2009) Abnormal megakaryocyte morphology and proplatelet formation in mice with megakaryocyte-restricted MYH9 inactivation. *Blood* 113:3182–3189.
13. Eckly A, et al. (2010) Proplatelet formation deficit and megakaryocyte death contribute to thrombocytopenia in Myh9 knockout mice. *J Thromb Haemost* 8:2243–2251.
14. Chen Z, et al. (2007) The May-Hegglin anomaly gene MYH9 is a negative regulator of platelet biogenesis modulated by the Rho-ROCK pathway. *Blood* 110:171–179.
15. Tsai RK, Discher DE (2008) Inhibition of "self" engulfment through deactivation of myosin-II at the phagocytic synapse between human cells. *J Cell Biol* 180:989–1003.
16. Thon JN, et al. (2010) Cytoskeletal mechanics of proplatelet maturation and platelet release. *J Cell Biol* 191:861–874.
17. Hategan A, Law R, Kahn S, Discher DE (2003) Adhesively-tensed cell membranes: Lysis kinetics and atomic force microscopy probing. *Biophys J* 85:2746–2759.
18. Guminski AD, Harnett PR, deFazio A (2001) Carboplatin and paclitaxel interact antagonistically in a megakaryoblast cell line—A potential mechanism for paclitaxel-mediated sparing of carboplatin-induced thrombocytopenia. *Cancer Chemother Pharmacol* 48: 229–234.
19. Italiano JE, Jr., Lecine P, Shivdasani RA, Hartwig JH (1999) Blood platelets are assembled principally at the ends of proplatelet processes produced by differentiated megakaryocytes. *J Cell Biol* 147:1299–1312.
20. Nilsson SK, et al. (1998) Immunofluorescence characterization of key extracellular matrix proteins in murine bone marrow in situ. *J Histochem Cytochem* 46:371–377.
21. Winer JP, Janmey PA, McCormick ME, Funaki M (2009) Bone marrow-derived human mesenchymal stem cells become quiescent on soft substrates but remain responsive to chemical or mechanical stimuli. *Tissue Eng Part A* 15:147–154.
22. Zutter MM, Painter AA, Staatz WD, Tsung YL (1995) Regulation of alpha 2 integrin gene expression in cells with megakaryocytic features: A common theme of three necessary elements. *Blood* 86:3006–3014.
23. Lagrue-Lak-Hal AH, et al. (2001) Expression and function of the collagen receptor GPVI during megakaryocyte maturation. *J Biol Chem* 276:15316–15325.
24. Pallotta I, Lovett M, Rice W, Kaplan DL, Balduini A (2009) Bone marrow osteoblastic niche: A new model to study physiological regulation of megakaryopoiesis. *PLoS ONE* 4:e8359.
25. Mahaut-Smith MP, et al. (2003) Properties of the demarcation membrane system in living rat megakaryocytes. *Biophys J* 84:2646–2654.
26. Dulyaninova NG, House RP, Betapudi V, Bresnick AR (2007) Myosin-IIA heavy-chain phosphorylation regulates the motility of MDA-MB-231 carcinoma cells. *Mol Biol Cell* 18:3144–3155.
27. Saito Y, Haendeler J, Hojo Y, Yamamoto K, Berk BC (2001) Receptor heterodimerization: Essential mechanism for platelet-derived growth factor-induced epidermal growth factor receptor transactivation. *Mol Cell Biol* 21:6387–6394.
28. Su RJ, et al. (2001) Platelet-derived growth factor enhances ex vivo expansion of megakaryocytic progenitors from human cord blood. *Bone Marrow Transplant* 27: 1075–1080.
29. Baba T, Fusaki N, Shinya N, Iwamatsu A, Hozumi N (2003) Myosin is an in vivo substrate of the protein tyrosine phosphatase (SHP-1) after mIgM cross-linking. *Biochem Biophys Res Commun* 304:67–72.
30. Raslova H, et al. (2007) Interrelation between polyploidization and megakaryocyte differentiation: A gene profiling approach. *Blood* 109:3225–3234.
31. Salles II, et al. (2009) Human platelets produced in nonobese diabetic/severe combined immunodeficient (NOD/SCID) mice upon transplantation of human cord blood CD34(+) cells are functionally active in an ex vivo flow model of thrombosis. *Blood* 114:5044–5051.
32. Fuentes R, et al. (2010) Infusion of mature megakaryocytes into mice yields functional platelets. *J Clin Invest* 120:3917–3922.
33. Di Pumpo M, et al. (2002) Defective expression of GPIb/IX/V complex in platelets from patients with May-Hegglin anomaly and Sebastian syndrome. *Haematologica* 87: 943–947.
34. Eto K, et al. (2002) Megakaryocytes derived from embryonic stem cells implicate CalDAG-GEFI in integrin signaling. *Proc Natl Acad Sci USA* 99:12819–12824.
35. Takayama N, et al. (2008) Generation of functional platelets from human embryonic stem cells in vitro via ES-sacs, VEGF-promoted structures that concentrate hematopoietic progenitors. *Blood* 111:5298–5306.
36. Smith, CM, 2nd, Burris SM, White JG (1989) Micropipette aspiration of guinea pig megakaryocytes: Absence of fragmentation and dependence on maturation stage. *Blood* 73:1570–1575.
37. Wilson CA, et al. (2010) Myosin II contributes to cell-scale actin network treadmilling through network disassembly. *Nature* 465:373–377.